

Deformation-based Strut-and-Tie Model for flexural members subject to transverse loading

Sung-Gul Hong^{1a}, Soo-Gon Lee^{2b}, Seongwon Hong^{1c} and Thomas H.-K. Kang^{*1}

¹Department of Architecture and Architectural Engineering, Seoul National University, 1 Gwanak-ro, Gwanak-gu, Seoul 08826, Republic of Korea

²Samsung C&T, 14 Seocho-daero 74-gil, Seocho-gu, Seoul 06620, Republic of Korea

(Received June 30, 2016, Revised August 28, 2016, Accepted September 7, 2016)

Abstract. This paper describes a deformation-based strut-and-tie model for the flexural members at post-yield state. Boundary deformation conditions by flexural post-yield response are chosen in terms of the flexural bar strains as the main factor influenced on the shear strength. The main purpose of the proposed model is to predict the shear capacities of the flexural members associated with the given flexural deformation conditions. To verify the proposed strut-and-tie model, the estimated shear strengths depending on the flexural deformation are compared with the experimental results. The experimental data are in good agreement with the values obtained by the proposed model.

Keywords: beam; deformation; strut-and-tie model; transverse loading; ultimate strength

1. Introduction

The flexural and shear capacities of the line components of structures including beams subjected to transverse loading are a primary concern when they are designed. The procedure of the structural analysis of an entire structure is as follows: The flexural design is first conducted so that their flexural capacities satisfy applied bending moments and then the shear strength is checked to be stronger than the shear forces associated with the flexural strength. Flexural design of the members is simply achieved by sectional analysis under the assumption of the plane section. However, despite the tremendous empirical or analytical studies (Bresler and Scordelis 1963; Kani *et al.* 1979; Anderson and Ramirez 1989; Reineck 1991; Collins *et al.* 1996; Choi *et al.* 2012; Kassem 2015; Lee *et al.* 2016), there are no shear strength models which were generally consented, and the conservative shear strength obtained from empirical works is used in current design. The shear strength of reinforced concrete members is known to be influenced by a number of factors, which include the concrete strength, the quantity of the shear reinforcement, the ratio of shear

*Corresponding author, Associate Professor, E-mail: tkang@snu.ac.kr

^aProfessor

^bStructural Engineer

^cPost-Doctoral Researcher

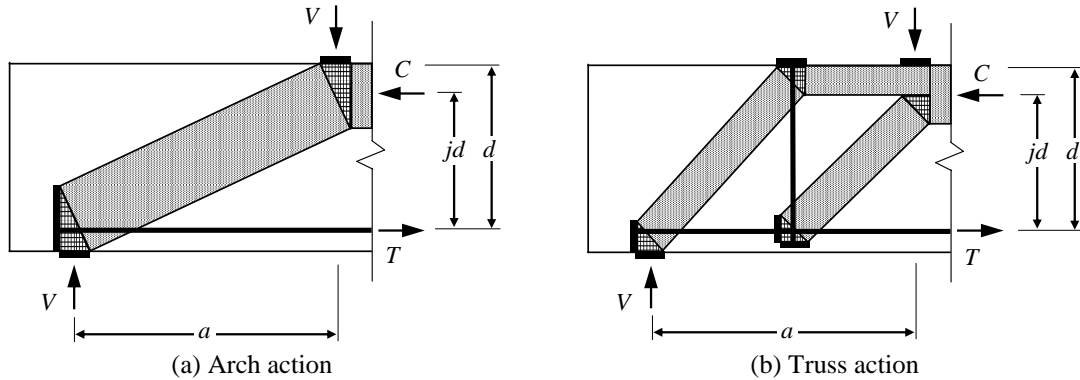


Fig. 1 Shear transfer mechanisms of deep beams: (a) arch action; (b) truss action

reinforcement to flexural reinforcement, and the ratio of shear span relative to section depth. In addition to these geometrical factors, however, deformation condition of the members can be also an important factor determining the shear strength because of the softening characteristics of concrete with the increase of the strain in transverse direction and the bond loss with yield penetration (Hong *et al.* 2011, 2016).

In this paper, a deformation-based strut-and-tie model for flexural members at the post-yield state is proposed. The deformation states of general beams are classified into five states. To validate the developed strut-and-tie model, the estimated shear strengths are compared with the experimental results. The experimental data show good agreement with the values estimated by the proposed model.

2. Deformation-based Strut-and-Tie model for deep beams

2.1 Shear transfer mechanism of deep beams

Fig. 1 shows a load path of shear forces in deep beams. Arch action signifies the shear transfer by direction of diagonal strut connecting from the loading to the support, while truss action denotes the shear transfer via the transverse tie. In general, the portions of arch and truss actions are known to be dependent upon the ratio of shear span to section depth a/d and the transverse reinforcement.

2.2 Strut-and-Tie modeling of deep beams

To present the deformation-based strut-and-tie models, the deformation states of the deep beams are categorized into four states with the model taken as a function of the strain of flexural bars at the loading section. First, the flexural bars remain elastic or embark yielding in the model for State-I. In State-II, the flexural bars yield and yield penetration begins to propagate. In State-III, flexural deformation is developed so that the length of yielding bars is over half the span length. The yield penetration of flexural bars is fully developed and then the bond stress disappears in State-IV. The states, as a general guide to construct the strut-and-tie models, are selected from the following equations. These equations are demonstrated in terms of the range of the strain value of

$$\left\{ \begin{array}{l} \varepsilon_{req} \leq \varepsilon_y \quad \text{for State-I} \\ \varepsilon_y < \varepsilon_{req} \leq \varepsilon_y + \frac{2f_{by}}{d_b E_{sh}} a \quad \text{for State-II} \\ \varepsilon_y + \frac{2f_{by}}{d_b E_{sh}} a < \varepsilon_{req} \leq \varepsilon_y + \frac{4f_{by}}{d_b E_{sh}} a \quad \text{for State-III} \\ \varepsilon_y + \frac{4f_{by}}{d_b E_{sh}} a < \varepsilon_{req} \quad \text{for State-IV} \end{array} \right. \quad (1)$$

the flexural bars at the loading section. where ε_{req} denotes the required strain of flexural bars at the loading section; ε_y is yield strain of steel; E_{sh} is the post-yield modulus of steel ($=1/20 E_s$); and f_{by} is the fictitious bond stress along the yielded bar ($=1/5 f_b$). The length of yielding bars is determined as

$$l_y = (\varepsilon_{req} - \varepsilon_y) \frac{d_b E_{sh}}{4f_{by}} \geq 0 \quad (2)$$

where d_b is the diameter of a flexural bar.

The guide for dividing the deformation states can be replaced in terms of the length of yield penetration l_y as follow

$$\left\{ \begin{array}{l} l_y = 0 \quad \text{for State-I} \\ 0 < l_y \leq \frac{a}{2} \quad \text{for State-II} \\ \frac{a}{2} < l_y < a \quad \text{for State-III} \\ l_y = a \quad \text{for State-IV} \end{array} \right. \quad (3)$$

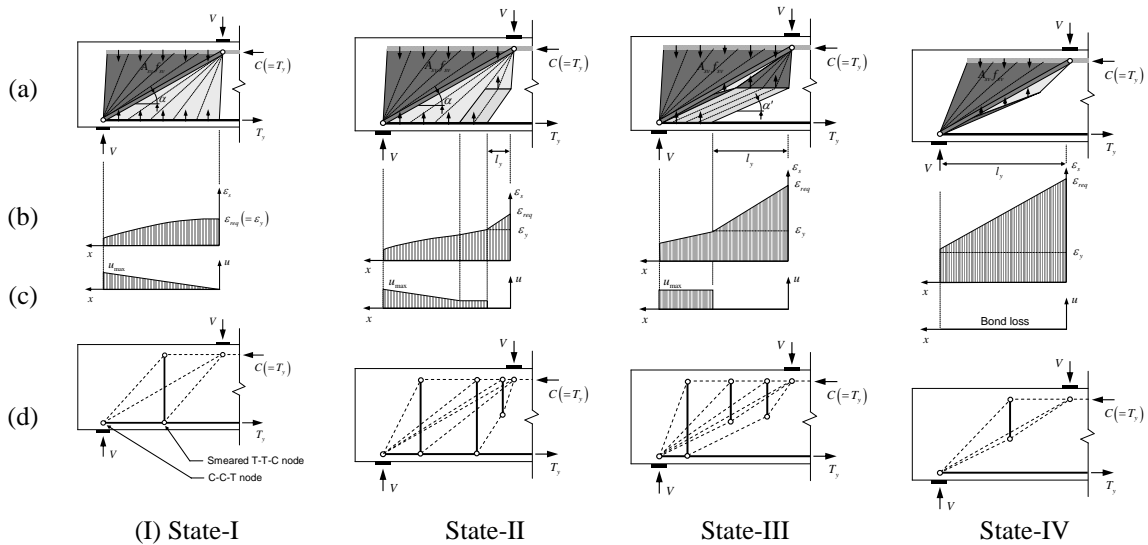


Fig. 2 Model for State-I to IV: (a) stress field; (b) strain distribution of flexural bar; (c) bond stress distribution; (d) strut-and-tie model

2.2.1 State-I: Before yielding or initial yielding

Fig. 2 exhibits the stress field for the deep beam. The distributions of flexural bar strain, bond stress, and the strut-and-tie model representing the load flows of the stress field are illustrated in Figs. 2(b), 2(c), and 2(d), respectively. In the stress field in Fig. 2(a), the maximum bond stress is determined to be at the support region. The maximum bond stress is calculated by the capacity of transverse tie and diagonal strut as follows

$$u_{\max} = \min \left(\begin{array}{l} \frac{A_{sv} f_{yv}}{s \tan \alpha} \frac{1}{n \pi d_b} \\ \frac{f_{ce} b \sin \alpha \cos \alpha}{n \pi d_b} \\ f_b \end{array} \right) \quad (4)$$

where n is the number of flexural bars; A_{sv} is the area of transverse reinforcement between a space s ; f_{yv} is the yield stress of transverse reinforcement; f_{ce} is the effective strength of the diagonal strut; b is the beam width; f_b is the bond strength ($= 2f_s \sin 2\theta$ ($0^\circ \leq \theta \leq 45^\circ$) for T-T-C node or $4f_i$ for C-C-T node); and the inclined angle α is determined as

$$\tan \alpha = \frac{jd}{a} \quad (5)$$

From the maximum bond stress in Eq. (5), the stress of transverse reinforcement is reversely found as

$$f_{sv} = \frac{n \pi d_b u_{\max} s \tan \alpha}{A_{sv}} \quad (6)$$

The stress of transverse reinforcement f_{sv} generally takes yield stress f_{yv} . However, Eq. (6) shows that in case where the bond stress u near the support reaches the strength f_b , the stress of transverse reinforcement f_{sv} is governed by bond strength.

Deformation of flexural tension reinforcement determines the flexural deformation of a deep beam. The average strain of the flexural reinforcement is a factor to determine the effective strength f_{ce} of a diagonal strut. With maximum bond stress u_{\max} in Eq. (4), the bond stress and the strain increment of flexural bars at the distance of x from the loading section are as follows

$$u = u_{\max} \frac{x}{a} \quad (7)$$

$$\frac{d\varepsilon_s}{dx} = -\frac{4u_{\max}}{d_b E_s a} x \quad (8)$$

The strain of the flexural bars at the distance of x from the loading point is calculated as in the following

$$\varepsilon_s = \varepsilon_{req} - \frac{2u_{\max}}{d_b E_s a} x^2 \quad (9)$$

Integrating the strain of the flexural bars over the span a , the entire tensile deformation of the

flexural bars δ_s are given by

$$\delta_s = \int_0^a \left(\varepsilon_{req} - \frac{2u_{\max}}{d_b E_s a} x^2 \right) dx = \left(\varepsilon_{req} - \frac{2au_{\max}}{3d_b E_s} \right) a \quad (10)$$

From Eq. (10), the average strain of the flexural bars can be calculated by the dividing the deformation by the span length a as

$$\varepsilon_{s,ave} = \frac{\delta_s}{a} \quad (11)$$

2.2.2 State-II: After yielding (small flexural deformation)

If the strain of the reinforcement at loading section exceeds the yield strain, yield penetration to the deep beam region is developed and the bond stress is diminished in the yielding zone (see Fig. 2). To carry the bond stress lost in the yielding zone, the fan-shaped region near the yielding zone changes into uniform stress field. The bond stress between the end of yielding zone and the twice of the yielding zone length from the loading section is uniformly distributed. In the other regions out of the twice of the yielding length from the loading section, the bond stress distribution is the same as that of the State-I. The maximum bond stress and stress of transverse reinforcement of State-II are not different from those of State-I. Eqs. (4), (5), and (6) are employed for State-II.

The bond stress and the strain increment of flexural bars at the distance of x from the loading section are as follows

$$u = \begin{cases} 0 & (x < l_y) \\ u_{\max} \frac{2l_y}{a} & (l_y \leq x < 2l_y) \\ u_{\max} \frac{x}{a} & (2l_y \leq x < a) \end{cases} \quad (12)$$

$$\frac{d\varepsilon_s}{dx} = \begin{cases} -\frac{4f_{by}}{d_b E_{sh}} & (x < l_y) \\ -\frac{8u_{\max} l_y}{d_b E_s a} & (l_y \leq x < 2l_y) \\ -\frac{4u_{\max}}{d_b E_s a} x & (2l_y \leq x < a) \end{cases} \quad (13)$$

The strain distribution of the flexural bars in the State-II can be determined by integrating the strain increment. Along the x-axis, the strain of the flexural bar is given by

$$\varepsilon_s = \begin{cases} \varepsilon_{req} - \frac{4f_{by}}{d_b E_{sh}} x & (x \leq l_y) \\ \varepsilon_y - \frac{8u_{\max} l_y}{d_b E_s a} (x - l_y) & (l_y \leq x < 2l_y) \\ \varepsilon_y - \frac{2u_{\max}}{d_b E_s a} x^2 & (2l_y \leq x < a) \end{cases} \quad (14)$$

The deformation of the flexural bars of the deep beam is calculated by integrating the strain over the span length as

$$\begin{aligned}\delta_s &= \int_0^{l_y} \left(\varepsilon_{req} - \frac{4f_{by}}{d_b E_{sh}} x \right) dx + \int_{l_y}^{2l_y} \left(\varepsilon_y - \frac{8u_{\max} l_y}{d_b E_s a} (x - l_y) \right) dx \\ &\quad + \int_{2l_y}^a \left(\varepsilon_y - \frac{2u_{\max}}{d_b E_s a} x^2 \right) dx \\ &= \varepsilon_{req} l_y + \varepsilon_y (a - l_y) - \frac{2f_{by}}{d_b E_{sh}} l_y^2 - \frac{2u_{\max}}{3d_b E_s a} (a^3 - 2l_y^3)\end{aligned}\quad (15)$$

The average strain of the flexural bars is calculated by dividing δ_s by span a .

2.2.3 State-III: Large flexural deformation

If the strain of main bars increases such that the yielding zone length l_y exceeds half the span length $a/2$, bond forces transferred in the smeared T-T-C nodal zone are gradually shifted to the C-C-T node at the support, as demonstrated in Fig. 2. In State-III, the maximum bond stress and the stress of transverse reinforcement should be changed to satisfy the change of the inclined strut angle near the support. The maximum bond stress is taken as

$$u_{\max} = \min \left(\begin{array}{l} \frac{A_{sv} f_{yv}}{s \tan \alpha'} \frac{1}{n\pi d_b} \\ \frac{f_{ce} b \sin \alpha' \cos \alpha'}{n\pi d_b} \\ f_b \end{array} \right) \quad (16)$$

where α' is the changed angle of the inclined strut connected with the non-yielding ties, which is defined as

$$\tan \alpha' = \frac{jd}{2l_y} \quad (17)$$

Note that if the inclined strut angle is changed in Eq. (17), the fan region must extend over the support point to carry the bond force lost in the yielding zone. Thus, another component to transfer the bond force, which cannot be carried by the T-T-C node, is required. That will be addressed with the condition of C-C-T nodal zone. From the maximum bond stress in Eq. (16), the stress of transverse reinforcement is reversely determined as

$$f_{sv} = \frac{n\pi d_b u_{\max} s \tan \alpha'}{A_{sv}} \quad (18)$$

In the same manner as the State-I or II, bond stress u and strain increment of distance x from the loading section is calculated as

$$u = \begin{cases} 0 & (x < l_y) \\ u_{\max} & (l_y \leq x < a) \end{cases} \quad (19)$$

$$\frac{d\varepsilon_s}{dx} = \begin{cases} -\frac{4f_{by}}{d_b E_{sh}} & (x < l_y) \\ -\frac{4u_{\max}}{d_b E_s} & (l_y \leq x < a) \end{cases} \quad (20)$$

The strain distribution of the flexural bars in the State-III can be determined by integrating the strain increment. Along the x -axis, the strain of the flexural bar is determined as

$$\varepsilon_s = \begin{cases} \varepsilon_{req} - \frac{4f_{by}}{d_b E_{sh}} x & (x \leq l_y) \\ \varepsilon_y - \frac{4u_{\max}}{d_b E_s} (x - l_y) & (l_y \leq x < a) \end{cases} \quad (21)$$

The deformation of the flexural bars of the deep beam is calculated by integrating the strain over the span length as

$$\begin{aligned} \delta_s &= \int_0^{l_y} \left(\varepsilon_{req} - \frac{4f_{by}}{d_b E_{sh}} x \right) dx + \int_{l_y}^a \left(\varepsilon_y - \frac{4u_{\max}}{d_b E_s} (x - l_y) \right) dx \\ &= \varepsilon_{req} l_y + \varepsilon_y (a - l_y) - \frac{2f_{by}}{d_b E_{sh}} l_y^2 - \frac{2u_{\max}}{d_b E_s} (a - l_y)^2 \end{aligned} \quad (22)$$

The average strain of the flexural bars is calculated by dividing δ_s by span a .

2.2.4 State-IV: Ultimate Flexural Deformation

In State-IV, the main bars over the span are fully yielded. The smeared T-T-C node having been in the flexural tie disappears and then only arch action resists the shear force. The State-IV represents the ultimate state in carrying the shear force of the deep beam. The transverse reinforcement just plays a part as confining of arch strut. The stress of transverse reinforcement is determined by only the capacity of the diagonal strut as

$$f_{sv} = \frac{f_{ce} b s \sin^2 \alpha}{A_{sv}} \quad (23)$$

In State-IV, the bond stress along the flexural bars is fully diminished.

$$u = 0 \quad (24)$$

The strain increment of the flexural bar is given by

$$\frac{d\varepsilon_s}{dx} = -\frac{4f_{by}}{d_b E_{sh}} \quad (25)$$

The strain distribution of the flexural bars in the State-III can be determined by integrating the strain increment. Along the x -axis, the strain of the flexural bar is given by

$$\varepsilon_s = \varepsilon_{req} - \frac{4f_{by}}{d_b E_{sh}} x \quad (26)$$

The deformation of the flexural bars of the deep beam is calculated by integrating the strain over the span length as

$$\delta_s = \varepsilon_{req} l_y - \frac{2f_{by}}{d_b E_{sh}} a^2 \quad (27)$$

The average strain of the flexural bars is calculated by dividing δ_s by span a .

2.3 Shear strength of deep beams

2.3.1 State-I and-II

In the State-I and II, shear strength of deep beams are determined by the summation of arch action V_a and truss action V_t as

$$V_u = V_a + V_t \quad (28)$$

The shear forces transferred by arch action V_a and truss action V_t are defined as follows

$$V_a = a_{arch} b f_{ce} \sin \alpha \quad (29)$$

$$V_t = \frac{A_{sv} f_{sv} a}{s} \quad (30)$$

where the strut width a_{arch} is determined from the capacity of C-C-T nodal zone at the support; and the effective strength f_{ce} is calculated in Eq. (31) with the following deformation conditions.

$$f_{ce} = \nu f'_c \quad (31)$$

where f'_c is the concrete compressive strength;

$$\nu = 0.85 \quad \text{for longitudinal strut} \quad (32)$$

$$\nu = \frac{1}{0.8 + 170\varepsilon_1} \leq 0.85 \quad \text{for diagonal strut} \quad (33)$$

$$\varepsilon_1 = \varepsilon_x + \varepsilon_v - \varepsilon_2 \quad (34)$$

To make easier, it is assumed that the direction of principal compression strain coincides with the direction of diagonal concrete strut. Since the model represents the ultimate state of shear transferring mechanism, the principal compression strain is taken as the strain at the ultimate stress.

$$\varepsilon_2 = \varepsilon_{cu} (= -0.002) \quad (35)$$

The average horizontal strain ε_x is taken as the half of the average strain of the flexural bars in Eq. (11) as below on the assumption that the horizontal compression strain of top chord is ignored.

$$\varepsilon_x = \frac{\varepsilon_{s,ave}}{2} \quad (36)$$

The vertical strain is simply taken by dividing the transverse tie stress by elastic modulus of steel.

$$\varepsilon_v = \frac{f_{sv}}{E_s} \quad (37)$$

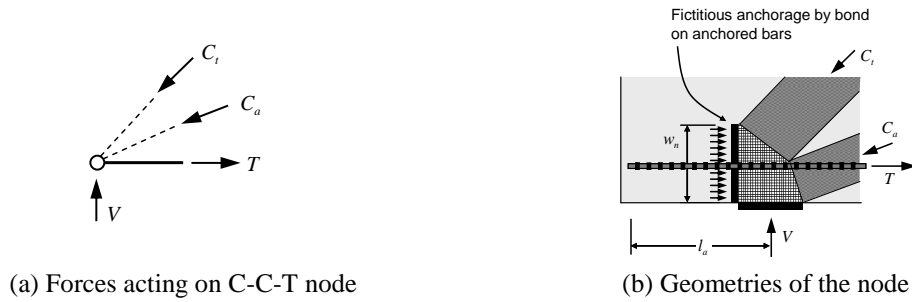


Fig. 3 C-C-T node: (a) forces acting on C-C-T node; (b) geometries of the node

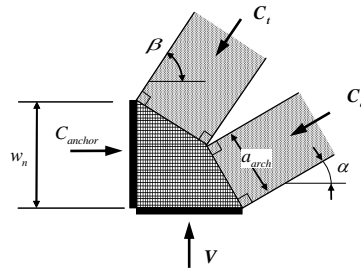


Fig. 4 Dimensions of C-C-T node

Fig. 3 shows (a) forces acting on the C-C-T node at support and (b) the geometries of the node. In the figure, the force C_t represents the compression force of fan region carrying the shear via the transverse ties and the force C_a denotes the compression force of arch strut. To ensure the transferring between the tensile force T in the flexural tie and compression forces in diagonal strut C_t and C_a , the load transferring capacity of the C-C-T node should be sufficiently achieved. In Figure 3(b), fictitious anchor plate is employed so as to determine the dimension and strength of the C-C-T nodal zone. In order to avoid the anchorage failure, sufficient anchorage length should be provided in the left side of the support. The anchorage length l_a is defined as the length between the support point and end of the bars. The nodal depth of C-C-T node w_n can be determined by assuming the anchorage zone as smeared C-C-T node where bond stress along the bars is $f_{bc} (=4f_t)$.

$$w_n = \frac{n\pi d_b f_{bc} l_a}{b(0.85 f'_c)} \left(< \frac{A_s f_y}{b(0.85 f'_c)} \right) \quad (38)$$

In the State-I or II, the dimensions of C-C-T node is defined as shown in Fig. 4. The compression forces C_t and C_a are determined as

$$C_t = \frac{A_{sv} f_{sv} a}{s \sin \beta} \quad (39)$$

$$C_a = a_{arch} b v f'_c \quad (40)$$

where β is the angle of the mean angle of fan-shaped strut composing truss action C_t as

$$\tan \beta = \frac{2jd}{a} \quad (41)$$

At the C-C-T node, equilibrium among the horizontal components of the anchorage force, the compression force C_t and the compression force C_a should be satisfied as

$$(0.85 f'_c) w_n b = C_t \cos \beta + C_a \cos \alpha \quad (42)$$

Thus, the depth of arch strut a_{arch} can be determined as

$$a_{arch} = \frac{w_n}{\cos \alpha} - \frac{C_t \cos \beta}{b(0.85 f'_c) \cos \alpha} \quad (43)$$

If the depth of diagonal strut a_{arch} has a negative value, the failure of a deep beam is governed by anchorage failure. In that case, the contribution of arch action becomes nullified and the truss action is also limited by anchorage capacity. Therefore, the shear strength governed by anchorage failure is given by

$$V_u = b w_n (0.85 f'_c) \tan \beta \quad (44)$$

2.3.2 State-III and IV

In the State-III and State-IV, shear resistance by truss action is gradually diminished and the role of transverse reinforcement is changed from truss action to the confining effect of the arch strut. From the strut-and-tie models in Fig. 2(d), the shear strength of deep beams in the State-III and IV is presented in the same form of those of the State-I or State-II as

$$V_u = V_a + V_t \quad (45)$$

The shear force transferred by arch action V_a is defined in the same manner with in State-I or II, as follows

$$V_a = a_{arch} b f_{ce} \sin \alpha \quad (46)$$

The strut width a_{arch} is determined from the C-C-T nodal condition at the support and the arch strut mid-depth as below

$$a_{arch} = \begin{cases} \frac{w_n}{\cos \alpha} - \frac{C_t \cos \beta}{b(0.85 f'_c) \cos \alpha} & \text{at C-C-T nodal face} \\ (a - 2l_y) \sin \alpha' & \text{at mid-strut} \end{cases} \quad (47)$$

where the compression force composing the truss action C_t is determined as

$$C_t = \frac{A_{sv} f_{sv}}{s \sin \beta} (2a - 2l_y) \quad (48)$$

The effective strength f_{ce} follows the effective strength of nodal face f_{cn} at the C-C-T node and Eq. (33) at the mid-strut with deformation conditions in the same manner with those in State I and State II. The shear resistance of arch action is determined as

$$V_a = \min \left\{ \begin{aligned} &a_{arch} b f_{ce} \sin \alpha = \left(\frac{w_n}{\cos \alpha} - \frac{C_t \cos \beta}{b(0.85 f'_c) \cos \alpha} \right) b f_{cn} \sin \alpha \\ &(a - 2l_y) b f_{ce} \sin \alpha' \sin \alpha \end{aligned} \right. \quad (49)$$

The shear resistance by truss action V_t should be reduced to satisfy the equilibrium condition in the updating stress field as

$$V_t = \frac{A_{sv} f_{sv}}{s} (2a - 2l_y) \quad (50)$$

At the C-C-T node, equilibrium among the horizontal components of the anchorage force, the compression force C_t and the compression force C_a should be satisfied as

$$(0.85 f'_c) w_n b = C_t \cos \beta + C_a \cos \alpha \quad (51)$$

In case of the State-III and IV, anchorage failure is apt to occur because the more tension force in reinforcement should be anchored. However, since the depth of arch strut is calculated from the anchorage capacity of C-C-T node in this proposed model, the anchorage failure is presented as the failure of arch strut. Note that the anchorage failure in the State-III and IV is associated with the compression failure of arch strut.

3. Deformation-based Strut-and-Tie model for general beams

In case that shear span to depth ratio a/d increases, uniform compression field between the two opposite fans should take place instead of direct arch strut. Fig. 5 shows the stress field of a typical simple supported beam, where fan region is near the loading point and the support, and uniform compression field is between the fan regions.

To determine the shear strength of the beam, the geometry of stress field should be defined. The region of fan and the arch strut angle is predefined by the dimensions of the deep beam that are shear span a and lever arm length jd , the diagonal strut angle α of general beam depends on the transverse reinforcement, bond capacity of main bars, compressive strength of diagonal strut as well as the dimensions of beam. The diagonal strut angle should be determined according to the failure mode of a beam. In this section, possible shear failure modes of general simple supported beams are classified and the strut-and-tie models for estimating the shear strengths of the beams are provided. Stress fields vary due to the governing failure modes and flexural deformation conditions.

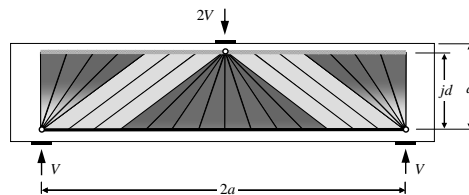


Fig. 3 Stress field of simple supported beam

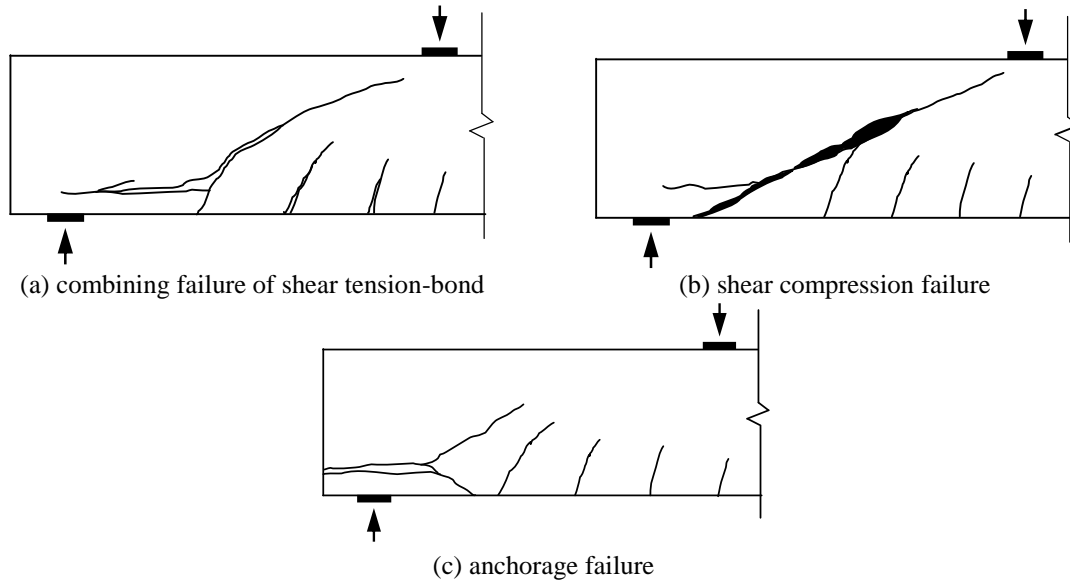


Fig. 4 Shear failure modes of general beams: (a) combining failure of shear tension and bond; (b) shear compression failure; and (c) anchorage failure

3.1 Classification of shear failure modes for beams

Relatively short beams with shear span to depth ratio a/d from 1 to 6 develop inclined cracks. The shear forces are carried by the concrete between the inclined cracks and transverse bars crossing the cracks. Due to redistribution of the internal forces, inclined crack angles are changed according to the loading stages. After forming the inclined cracks joining the support and the loading point, a part of shear force can be carried by arch action. In such a beam, shear failure modes are divided into four types: combining failure of shear tension and bond, shear compression failure and anchorage failure, which are illustrated in Fig. 6.

If the strut angle is defined and the strength reduction by flexural deformation is ignored, the shear strengths according to each failure mode can be determined by equilibrium condition and strengths of the component, as follows

- (1) Shear tension failure at inclined crack

$$V_{ST} = \frac{A_{sv} f_{yv} jd}{s \tan \alpha} \quad (52)$$

- (2) Bond failure along the main bars

$$V_B = jd n \pi d_b f_b \quad (53)$$

- (3) Shear compression failure at the uniform stress field

$$V_{SC} = b jd f_{ce} \sin \alpha \cos \alpha \quad (54)$$

- (4) Anchorage failure at the support

$$V_{An} = b w_n (0.85 f'_c) (2 \tan \alpha) \quad (55)$$

3.2 Shear strength of general beam

In the same manner as deep beams, stress fields for general beams are presented and categorized into five states according to the strain state of flexural bars at the loading section. First, in the model for the State-I, flexural bars remain elastic or embark yielding. In the State-II, flexural bars yield and yield penetration begins to propagate. In the State-III, flexural deformation has developed such that the length of yielding bars l_y exceeds half the initial fan shaped region. In the State-IV, the length of yielding bars l_y exceeds half the span $a/2$. In the State-V, the main bars yield over the span and the bond stress is fully deteriorated. The states, as a general guide to construct models, may be selected from the following equation

$$\left(\begin{array}{l} \varepsilon_{req} \leq \varepsilon_y \quad \text{for State I} \\ \varepsilon_y < \varepsilon_{req} \leq \varepsilon_y + \frac{2f_{by}}{d_b E_{sh}} \frac{jd}{\tan \alpha} \quad \text{for State II} \\ \varepsilon_y + \frac{2f_{by}}{d_b E_{sh}} \frac{jd}{\tan \alpha} < \varepsilon_{req} \leq \varepsilon_y + \frac{2f_{by}}{d_b E_{sh}} a \quad \text{for State III} \\ \varepsilon_y + \frac{2f_{by}}{d_b E_{sh}} a < \varepsilon_{req} \leq \varepsilon_y + \frac{4f_{by}}{d_b E_{sh}} a \quad \text{for State IV} \\ \varepsilon_y + \frac{4f_{by}}{d_b E_{sh}} a < \varepsilon_{req} \quad \text{for State V} \end{array} \right. \quad (56)$$

It also can be presented in terms of the yielding zone length l_y , as follows

$$\left(\begin{array}{l} l_y = 0 \quad \text{for State I} \\ 0 < l_y \leq \frac{jd}{2 \tan \alpha} \quad \text{for State II} \\ \frac{jd}{2 \tan \alpha} < l_y \leq \frac{a}{2} \quad \text{for State III} \\ \frac{a}{2} < l_y < a \quad \text{for State IV} \\ l_y = a \quad \text{for State V} \end{array} \right. \quad (57)$$

3.2.1 State-I: Before yielding

Fig. 7(a) shows the stress field for beams in the State-I, where shear tension failure would occur with bond failure or shear compression failure; shear tension-bond failure and shear tension-compression failure. Fig. 7(b) and (c) display the stress field and bond stress distribution along the main bars in the State-I, respectively, where the angle of uniformly distributed stress field α can be calculated by the condition of simultaneous failure of two components.

If the transverse reinforcement yields and the bond stress along the main bars reaches the

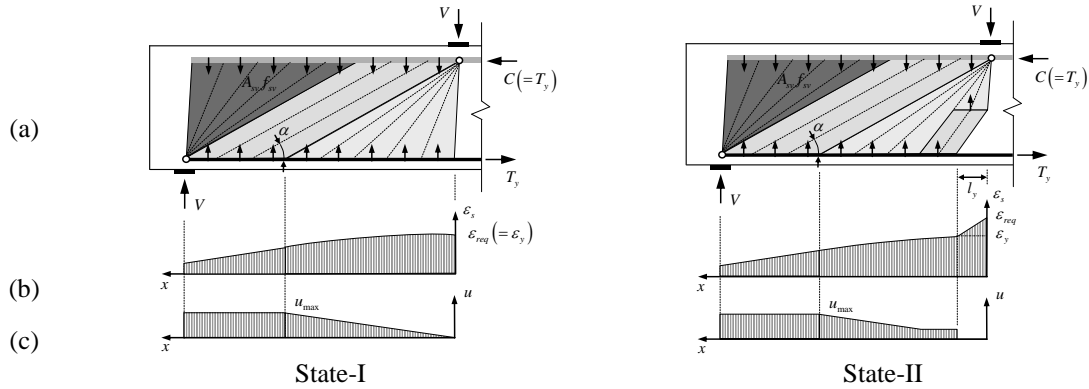


Fig. 7 Model for State-I and State-II: (a) stress field; (b) strain distribution of flexural bars; and (c) bond stress distribution along the flexural bars

strength, shear tension-bond failure occurs. From the condition of simultaneous yielding of transverse tie and bond failure at T-T-C node, the following equation is given

$$\frac{A_{sv} f_{yv} j d}{s \tan \alpha} = n \pi d_b f_b j d \tag{58}$$

If the transverse reinforcement is yielded and the compression stress of the uniformly distributed field reaches the effective strength, shear tension-compression failure occurs. From the condition of simultaneous yielding of transverse tie and crushing of diagonal strut, the following equation is given

$$\frac{A_{sv} f_{yv} j d}{s \tan \alpha} = b j d f_{ce} \cos \alpha \sin \alpha \tag{59}$$

If the inclined strut angle α obtained from Eqs. (58) and (59) is smaller than the angle from horizontal axis to the line joining load and support, uniformly distributed stress field does not form and the strength of a beam is determined from the stress field for deep beams, when the angle of inclined strut is given by

$$\tan \alpha = \frac{j d}{a} \tag{60}$$

The inclined strut angle in the State-I is determined as the minimum of the angles in Eqs. (58), (59) and (60). The governing failure mode of beam is determined by the inclined strut angle.

$$\alpha = \min. \text{ of } \begin{cases} \sin^{-1} \sqrt{\frac{A_{sv} f_{yv}}{4 s n \pi d_b f_t}} & \text{shear tension-bond failure} \\ \sin^{-1} \sqrt{\frac{A_{sv} f_{yv}}{s b f_{ce}}} & \text{shear tension-compression failure} \\ \tan^{-1} \left(\frac{j d}{a} \right) & \text{deep beam} \end{cases} \tag{61}$$

3.2.2 State-II: After yielding (small deformation)

In the stress field in the State-II, inclined strut angle does not change but the effective strength of concrete strut decreased due to the flexural deformation, as demonstrated in Fig. 7. The shear strength in the State-II is the same as that in the State-I, and is expressed as

$$V_u = \frac{A_{sv} f_{sv} j d}{s \tan \alpha} \tag{62}$$

where the stress of transverse reinforcement f_{sv} is limited by the equilibrium with diagonal strut forces as

$$f_{sv} = \frac{s b f_{ce} \sin^2 \alpha}{A_{sv}} \leq f_{yv} \tag{63}$$

The effective strength f_{ce} is calculated in Eqs. (31), (32), (33), and (34).

3.2.3 State-III: When yielding zone exceeds half of fan region

If flexural deformation increases so that the yielding zone length l_y exceeds half the fan length, the fan region extends with reduced inclined angle α' to carry the bond forces lost in previous fan region and stress field is then modified in Figure 8. Thus, the shear strength in the State-III is determined as

$$V_u = \frac{A_{sv} f_{sv} j d}{s \tan \alpha'} \tag{64}$$

Since the inclined strut angle decreases with the extension of yielding zone, the tensile stress of transverse reinforcement becomes under the yield stress which is calculated by equilibrium condition with inclined strut force and bond force as

$$f_{sv} = \min. \text{ of } \begin{cases} \frac{s b f_{ce} \sin^2 \alpha'}{A_{sv}} & \text{compression failure} \\ \frac{s n \pi d_b f_b \tan \alpha'}{A_{sv}} & \text{bond failure} \end{cases} \tag{65}$$

The effective strength f_{ce} is calculated using Eqs. (31), (32), (33), and (34).

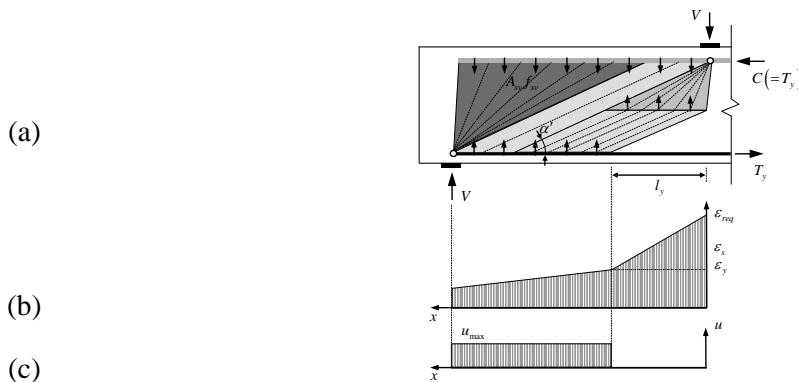


Fig. 8 Model for State-III: (a) stress field; (b) strain distribution of flexural bars; and (c) bond stress distribution along the flexural bars

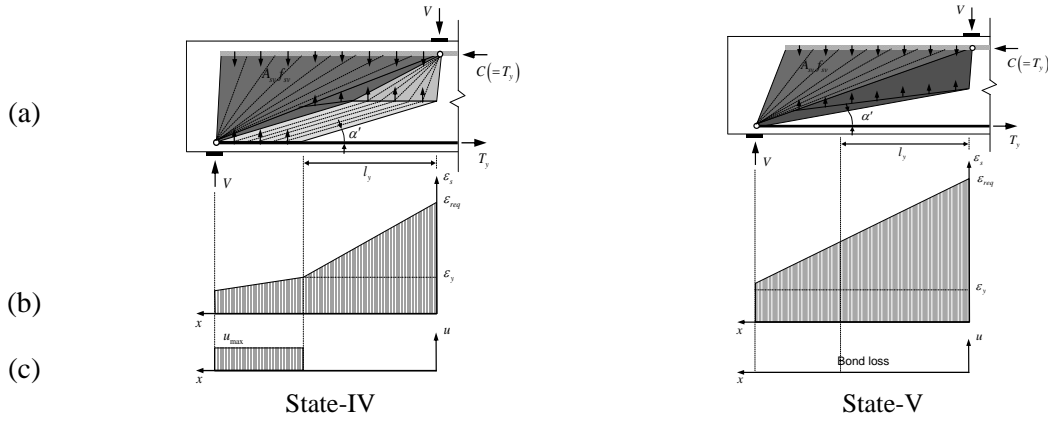


Fig. 9 Model for State-IV and State-V: (a) stress field; (b) strain distribution of flexural bars; and (c) bond stress distribution along the flexural bars

3.2.4 State-IV and V: When yielding zone exceeds half of span

If the inclined strut angle α' decreases so that the fan region length reaches the span length, an arch strut forms connecting the support and the loading point like the stress field of deep beams. Figure 9 shows the stress fields in the State-IV and V. The shear strength in the State-IV and V can be calculated by the procedures of deep beams in the State-III and IV, respectively.

3.2.5 Anchorage failure

Regardless of flexural deformation, anchorage failure may occur if sufficient development length over the support is not achieved. This anchorage failure should be checked for the stress fields at all states illustrated in the previous sections. The strength of anchorage failure is given by

$$V_u = bw_n (0.85 f'_c) \tan \beta \tag{66}$$

where the strut angle β is as follows

$$\tan \beta = \begin{cases} 2 \tan \alpha & \text{for State I, II} \\ 2 \tan \alpha' & \text{for State III} \\ \frac{2jd}{a} & \text{for State IV, V} \end{cases} \tag{67}$$

3.3 Summary of shear failure modes

Table 1 summarizes shear failure modes and guide for appropriate selection of the stress field according to the geometries and loading states of the beams. In elastic state (State-I), shear failures are accompanied with the yielding of shear reinforcement; (1) yielding of shear reinforcement and bond failure or (2) yielding of shear reinforcement and crushing of web concrete. Since the shear capacity associated with bond strength does not depend on the flexural deformation, bond failure could occur only before flexural yielding. At post-yield state, only the failure of compression strut causes the shear failure of the beam.

Table 1 Guide for appropriate selection of the model according to loading states

	Bond failure mode	Compression failure mode	Deep beam (arch strut failure)
State-I $l_y = 0$	α : Eq. (59) V_u : Eq. (53) Shear tension-bond failure	α : Eq. (60) V_u : Eq. (54) Shear tension-compression failure	α : Eq. (5) V_u : Eq. (28) Shear tension and arch strut failure
State-II $0 < l_y \leq \frac{l_f}{2}$			
State-III $\frac{l_f}{2} < l_y \leq \frac{a}{2}$		α :Eq. (65) V_u : Eq. (54) Shear compression failure by concrete softening	
State-IV $\frac{a}{2} < l_y < a$			α : Eq. (17) V_u : Eq. (45) Arch strut failure
State-V $l_y = a$			

4. Verification

4.1 Relationship between flexural deformation of beam and required strain of flexural bars at loading section

The stress fields and strut-and-tie models for beam shear strength proposed in this paper were based on the boundary deformation condition in terms of required strain of the flexural bars at the loading section. Because the boundary deformation is affected by the deformation of beam or the plastic hinge rotation, the strain of flexural bars is expressed in terms of flexural deformation of the beam.

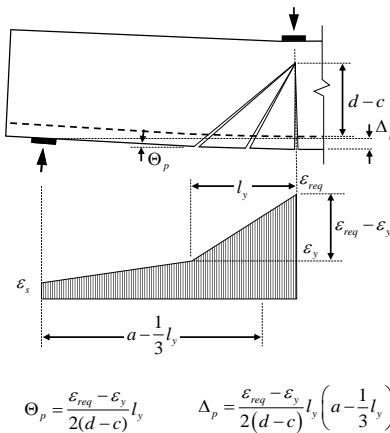


Fig. 5 Calculation of plastic flexural deformation of beam

For the relationship between vertical displacement of a beam at the mid-span and the strain of the flexural bars, the flexural deformation of a beam is subdivided into elastic deformation and plastic deformation. The vertical displacement of the mid-span Δ is expressed as

$$\Delta = \Delta_e + \Delta_p \tag{68}$$

where Δ_e is vertical displacement by the elastic flexural deformation of beam, which is calculated by following the ACI 318-14, as

$$\Delta_e = \frac{Va^3}{3E_c I_{eff}} \tag{69}$$

where V is the shear force applied on the beam; I_{eff} is the effective moment of inertia, which is selected as the equation proposed by ACI code. Note that the shear force V is not the shear strength of the strut-and-tie model but the shear force associated with flexural strain at the loading section.

$$V = \begin{cases} \frac{jd}{a} A_s E_s \varepsilon_{req} & \varepsilon_{req} < \varepsilon_y \\ \frac{jd}{a} A_s f_y & \varepsilon_{req} \geq \varepsilon_y \end{cases} \tag{70}$$

where Δ_p is the vertical displacement of beam by plastic strain of main bars within the yielding zone. As shown in Figure 10, plastic deformation is calculated as

$$\Delta_p = \frac{\varepsilon_{req} - \varepsilon_y}{2(d - c)} l_y \left(a - \frac{1}{3} l_y \right) \tag{71}$$

4.2 Comparison of the model prediction with test data

The proposed deformation-based strut-and-tie model for beams is used to calculate the shear strengths depending on the flexural deformation of total nine test specimens in the literature (Shin *et al.* 1999; Vecchio and Shim 2004). All tested beams were simply supported beams subjected to one point monotonic loading. In selecting the test data, the specimens that exhibited shear failure mode were considered. To consider the bond in T-T-C node composing the truss action, the beams without

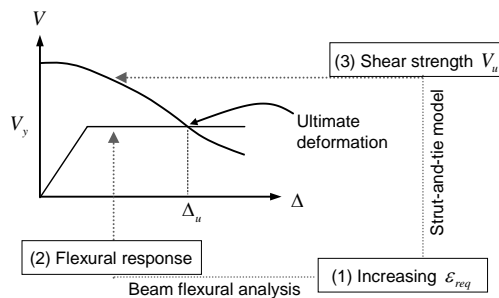


Fig. 6 Procedures determining ultimate deformation

Table 2 Dimensions and sectional properties of test specimens (Shin *et al.* 1996; Vecchio and Shim 2004)

Specimen	b (mm)	d (mm)	h (mm)	a (mm)	a/d
HB1.5-25	125	215	250	323	1.5
HB2.0-25	125	215	250	430	2
HB2.5-25	125	215	250	538	2.5
A1	305	457	552	1830	4
A2	305	457	552	2285	5
A3	305	457	552	3200	7
B1	229	457	552	1830	4
B2	229	457	552	2285	5
B3	229	457	552	3200	7
C1	152	457	552	1830	4
C2	152	457	552	2285	5
C3	152	457	552	3200	7

Notes: b is the beam width; d is the effective depth; h is the beam depth; a is the shear span length.

Table 3 Material properties and reinforcement information (Shin *et al.* 1996; Vecchio and Shim 2004)

Specimen	Concrete	Flexural Reinforcement		Vertical Reinforcement		
	f'_c (MPa)	A_s (mm ²)	f_y (MPa)	A_{sv} (mm ²)	f_{yv} (MPa)	s (mm)
HB1.5-25	73	982	414	56.5	414	101
HB2.0-25	73	982	414	56.5	414	141
HB2.5-25	73	982	414	56.5	414	188
A1	22.6	2400	440	64.4	600	210
A2	25.9	3100	440	64.4	600	210
A3	43.5	3800	440	51.4	600	168
B1	22.6	2400	440	64.4	600	190
B2	25.9	2400	440	64.4	600	190
B3	61.5	3100	440	51.4	600	152
C1	22.6	1400	440	64.4	600	210
C2	25.9	2400	440	64.4	600	210
C3	43.5	2400	440	51.4	600	168

Notes: f'_c is the concrete compressive strength; A_s is the area of reinforcement; f_y is the yield strength of reinforcing steel; A_{sv} is the area of vertical reinforcement; f_{yv} is the yield strength of vertical reinforcing steel; s is the spacing of shear reinforcement.

stirrup were not used for prediction. The geometries of the tested beams, the material properties, and the reinforcement information are summarized in Table 2 and 3. The tested beams cover a wide range of span conditions exhibiting the shear failure mode. The ratio of shear span to sectional effective depth a/d varies from 1.5 to 7. Using the proposed strut-and-tie model, the shear capacity of the beam is calculated with incrementally increasing flexural deformation. The ultimate deformation is obtained when the shear capacity decreases to the applied shear force

associated with flexural moment. The procedures determining the ultimate flexural deformation are summarized as below and conceptually illustrated in Fig. 11.

Table 4 Comparisons of strength and deformation with test results (Shin *et al.* 1996; Vecchio and Shim 2004)

Specimen	Test Result		Proposed Model		Comparison(cal/test)	
	$V_{u, test}$ (kN)	$\delta_{u, test}$ (mm)	$V_{u, cal}$ (kN)	$\delta_{u, cal}$ (mm)	$V_{u, cal}/V_{u, test}$	$\delta_{u, cal}/\delta_{u, test}$
HB1.5-25	211.6	2.68	192.8	1.17	0.911	0.438
HB2.0-25	145.1	3.07	151.6	1.78	1.045	0.581
HB2.5-25	120.4	3.33	123.1	2.79	1.022	0.838
A1	229.5	18.80	211.7	16.30	0.922	0.867
A2	219.5	29.10	212.1	31.33	0.966	1.077
A3	210.0	51.00	200.1	69.74	0.953	1.367
B1	217.0	22.00	194.5	17.37	0.896	0.789
B2	182.5	31.60	162.8	32.35	0.892	1.024
B3	171.0	59.60	170.5	76.87	0.997	1.290
C1	141.0	21.00	118.3	15.03	0.839	0.716
C2	145.0	25.70	138.3	33.71	0.954	1.312
C3	132.5	44.30	119.8	60.32	0.904	1.362

Notes: $V_{u, test}$ is the shear strength of specimen; $\delta_{u, test}$ is the deformation at failure; $V_{u, cal}$ is the calculated shear strength; $\delta_{u, cal}$ is the calculated deformation at failure.

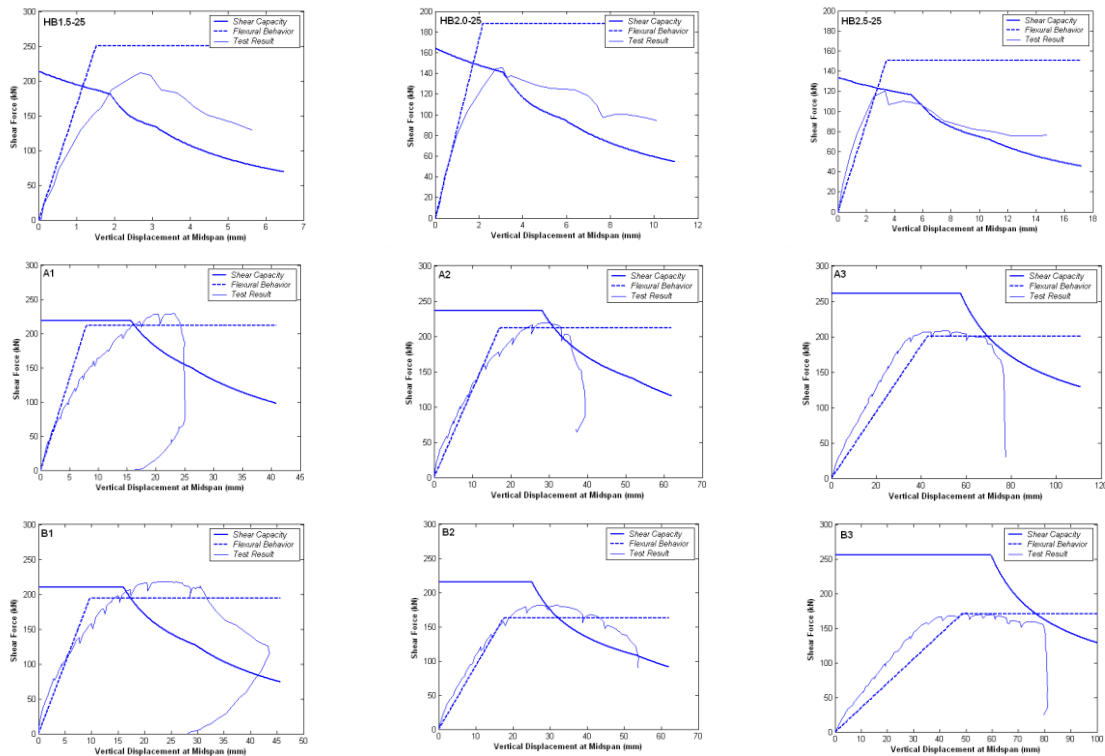


Fig. 12 Comparison of test results with predicted results

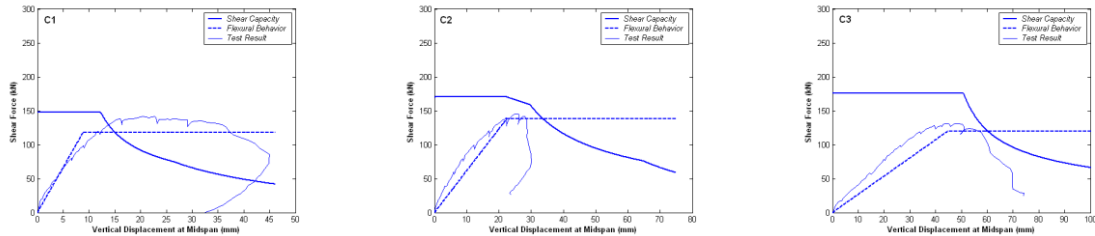


Fig. 12 Continued

(1) Determine the governing failure mode in elastic state from Eqs. (58), (59), and (60). This enables to determine the initial shear capacity and inclined strut angle α .

(2) Increase the required strain ε_{req} of flexural bars at the loading section.

(3) Calculate the applied shear force V and the flexural deformation Δ associated with the flexural bar strain ε_{req} from Eqs. (68), (69), (70), and (71). These shear force and flexural deformation govern the flexural response of the beam.

(4) Determine shear strength using the proposed strut-and-tie model according to the required strain ε_{req} . It is required to select the loading state from Eq. (56). The shear capacity can be calculated from the stress field corresponding to the selected loading state. In design, since the deformation requirement is given, shear reinforcement can be detailed in this step.

(5) Compare the applied shear force in step (3) and the shear strength in step (4). If the shear strength decreases to the applied shear force, shear failure occurs, and the flexural deformation is the ultimate flexural deformation of the beam. Repeat from step (2) to step (5) until the shear failure occurs.

Comparison of the predicted results with test data is illustrated in Fig. 12. The x-axis denotes the vertical displacement of beams and y-axis signifies the shear forces. The normal solid line illustrates the load-deformation relationship of the tested beam, the dashed line denotes the flexural response calculated from the deformation condition, and the bold solid line is the predicted shear strengths according to the flexural deformations using the proposed model. The intersection point of the shear strength (bold solid line) and flexural response (dashed line) indicates the flexural deformation capacity of the beam limited by shear failure.

5. Conclusions

In this paper, the procedure to determine the shear strength of beams at post-yield state depending on the flexural deformation is presented. Using strut-and-tie models capable of considering the change of stress field due to the redistribution of internal forces by the effect of flexural deformation at post yield state, flexural deformation capacity limited by shear failure can be predicted. The conceptual relationship between the shear capacity and the flexural behavior of beams is shown. As flexural deformation increases, shear strength of beams decreases. The point where the curve of flexural behavior meets the curve of shear capacity means shear failure limiting the flexural behavior. If requirement of flexural deformation is determined from the system analysis, the shear design can be carried out with the proposed deformation-based strut-and-tie model so that shear strength at required deformation state is larger than the shear force associated with flexural strength.

Acknowledgments

The work presented in this paper was supported in part by Interdisciplinary Research Grants (R01-2004-000-10290-0), in part by the National Research Foundation of Korea (NRF) grant (No. 2015-055508), and in part by the Engineering Research Institute at Seoul National University. The opinions, findings and conclusions in this paper are those of the writers and do not necessarily represent those of the sponsors.

References

- ACI Committee 318 (2014), Building code requirements for structural concrete (ACI 318-14) and commentary (ACI 318R-14), *Farmington Hills, Mich.*: American Concrete Institute, 520.
- Aderson, N.S. and Ramirez, J.A. (1989), "Detailing of stirrup reinforcement", *ACI Struct. J.*, **86**(5), 507-515.
- Bresler, B. and Scordelis, A.C. (1963), "Shear strength of reinforced concrete beams", *ACI J. Proceedings*, **60**, 51-74.
- Choi, Y.W., Lee, H.K., Chu, S.B., Cheong, S.H. and Jung, W.Y. (2012), "Shear behavior and performance of deep beams made with self-compacting concrete", *Int. J. Concrete Struct. Mater.*, **6**(2), 65-78.
- Collins, M.P., Mitchell, D., Adebar, P. and Vecchio, F.J. (1996), "A general shear design method", *ACI Struct. J.*, **93**(1), 36-45.
- Hong, S.G., Lee, S.G. and Kang, T.H.K. (2011), "Deformation-based Strut-and-Tie model for interior joints of frames subject to load reversal", *ACI Struct. J.*, **108**(4), 423-433.
- Hong, S.G., Lee, S.G., Hong, S. and Kang, T.H.K. (2016), "Deformation-based Strut-and-Tie Model for reinforced concrete columns subject to lateral loading", *Comput. Concrete*, **17**(2), 157-172.
- Kani, M.W., Huggins, M.W. and Wittkopp, R.R. (1979), "Kani on shear in reinforced concrete", Toronto: University of Toronto Dept. of Civil Engineering, 225.
- Kassem, W. (2015), "Strength prediction of corbels using strut-and-tie model analysis", *Int. J. Concrete Struct. Mater.*, **9**(2), 255-266.
- Lee, J.D., Yoon J.K. and Kang, T.H.K. (2016), "Combined half precast concrete slab and post-tensioned slab topping system for basement parking structures", *J. Struct. Integrity Maintenance*, **1**(1), 1-9.
- Reineck, K.H. (1991), "Ultimate shear force of structural concrete members without transverse reinforcement derived from a mechanical model (SP-885)", *ACI Struct. J.*, **88**(5), 592-602.
- Shin, S.W., Lee, K.S., Moon, J.I., and Ghosh, S.K. (1999), "Shear strength of reinforced high-strength concrete beams with shear span-to-depth ratios between 1.5 and 2.5", *ACI Structural Journal*, **96**(4): pp. 549-556.
- Vecchio, F.J. and Collins, M.P. (1986), "The modified compression field theory for reinforced concrete elements subjected to shear", *ACI J.*, **83**(2), 219-231.